7.1. Introduction

Quality by Design (QbD) involves systemic development of the formulation to develop quality product. The evaluation or characterization of the prepared formulation is the integral part of the QbD based formulation development process. Various characterization parameters like drug entrapment efficiency, drug loading, vesicle size, zeta potential, in vitro drug release, morphology were considered for the present investigation. Both the formulations i.e. PTX-UDNVs and CBP-UDNVs were characterized for these parameters.

7.2. Materials and Equipment

Materials

HPLC grade methanol (MeOH) and acetonitrile (ACN) were procured from Fisher Scientific (Vadodara, Gujarat) to carry out chromatographic analysis. Double distilled water used in the study was filtered using 0.22 micron nylon filter, Nylon N66 membrane filters 47 mm, Rankem, India. 0.1 micron Isopore polycarbonate membrane filters; 25 mm, VCTP02500; Sigma Aldrich, All other reagents were purchased from S.D. finechem Ltd, India and were of analytical grade.

Equipment

- Electronic weighing balance (ELB300, Shimadzu, Japan)
- Vortex Mixer (Spinix-Vortex Shaker, Tarsons, India)
- Ultrasonic Bath Sonicator (Ultrasonics Selec, Vetra, Italy)
- Rotary evaporator (IKA RV10, Karnataka, India)
- Probe Sonicator (LabsonicM, Sartorius Ltd, Mumbai, India)
- Cooling Centrifuge (Remi Equipment, Mumbai, India)
- HPLC (Shimadzu LC-20AT, Japan)
- Zeta sizer (Nano ZS Malvern Instruments, UK)
- Nikon H600L Microscope (Nikon, Japan)

7.3. Characterization of PTX-UDNVs

7.3.1. Methods

7.3.1.1. Vesicle Size and Zeta Potential

Briefly, vesicular dispersion was taken (50 µL) and diluted it with 2 ml of distilled water in order to obtain proper vesicle density. The dispersion thus prepared was filled in clear disposable sizing cuvettes and the mean hydrodynamic diameter and poly-dispersity index (PDI) were measured in triplicate by dynamic light scattering using Nano-ZS zetasizer. For the measurement of Zeta Potential, the diluted dispersion was transferred to disposable folded capillary cells and analysed for zeta potential using Nano-ZS zetasizer.

7.3.1.2. Entrapment efficiency and Drug loading

PTX loaded vesicular dispersion was centrifuged at 5000 RPM for 10 min to separate un-entrapped drug in sediment. The supernatant was separated and methanol was added to it in order to dissolve the lipids and to extract drug in solution. The amount of PTX was estimated by high performance liquid chromatography technique at 227 nm as described in Chapter 3 [1].

The entrapment efficiency and drug loading were calculated using following formula-

$$\%\ Entrapment\ Efficiency\ = \frac{Estimated\ Entrapped\ drug}{Total\ drug\ added\ to\ formulation} \times 100$$

$$\%\ Drug\ Loading\ (\%w/w) = \frac{Estimated\ Entrapped\ drug}{Total\ weight\ of\ formulation} \times 100$$

7.3.1.3. Deformability of the vesicles

The deformability of the phospholipid bilayer of PTX-UDNVs formulation and conventional liposomes was assessed using membrane extrusion method. For the measurement of deformability of the nano-vesicles, formulations were extruded at constant pressure through the 25 mm diameter Isopore polycarbonate filter membrane having a pore diameter of 100 nm. The amount of vesicle dispersion that was extruded during 5 min was measured, and the vesicle was monitored before and

after extrusion. The deformability of the nano-vesicles was measured using following equation [2]:

$$DI = J \times \left(\frac{R_v}{R_p}\right)^2$$

Where, *DI*= Deformability Index;

J= Amount of dispersion extruded (ml);

R_v= Vesicles size after extrusion (nm); and

R_p= Pore size of the barrier (nm)

7.3.1.4. Shape and surface morphology using TEM

The optimized formulation was evaluated for morphological properties using transmission electron microscopy (TEM). The vesicular dispersion was spread on a carbon-coated grid, excess solution was removed and the grid was dried under infrared lamp. 2% phosphotungstic acid (PTA) was used for negative staining and again dried under Infrared lamp. Transmission electron microscope (CM 200, Philips, Netherlands) with operating voltage range of 20-200 kV was used to visualize vesicles at suitable enlargement with an accelerating voltage of 20 kV.

7.3.1.5. In Vitro drug release study

In vitro release of drug from PTX-UDNVs were evaluated by the dialysis bag diffusion technique in phosphate buffer pH 4.5 with 1% SLS. The aqueous UDNVs dispersion equivalent to 2 mg of drug was placed in activated dialysis membrane (MWCO- 12000, Hi media, India) closed at one end using clamp. The other end was also closed using clamp and whole bag was immersed in beaker containing 50 ml phosphate buffer pH 4.5 with 1% SLS which was stirred at 100 rpm and maintained at 37 ± 1 °C throughout the experiment. At predetermined time intervals, 2 ml samples were withdrawn from the receptor compartment (media) and sink conditions were maintained by addition of similar quantities of fresh media. The samples were analysed for amount of drug released using previously described HPLC method. All the experiments were

performed in triplicate. Plain drug suspension prepared in 1% SLS solution was used as a control for comparison of drug release profile [3].

In vitro drug release from Intra Vaginal Rod (IVR) inserts was performed in similar method as described above. The IVR containing freeze-dried rod of the formulation was placed in the diffusion medium (phosphate buffer pH 4.5) maintained at 37 ± 1 °C and 100 rpm speed was kept constant. 2 ml samples were withdrawn from the receptor compartment (media) and sink conditions were maintained by addition of fresh media. The samples were analysed for amount of drug released using previously described HPLC method. All the experiments were performed in triplicate.

7.3.1.6. Permeation and Deposition study

The tissue permeation of PTX-UDNVs and plain drug suspension was determined Ex Vivo across Porcine Vaginal Membrane [4]. The porcine vaginal tissue was obtained immediately after animal sacrifice in a local slaughterhouse and preserved in the isotonic sodium chloride solution. Tissue was rinsed three times with saline solution, separated from the underneath connective tissues, and mounted between donor and receptor compartment of Franz's diffusion cell with 1.9 cm^2 effective diffusion area and 15 mL receptor chamber volume. The receptor compartment was filled with 1% SLS in PBS (pH 7.4) with constant stirring at 100 rpm. The vaginal membrane was carefully mounted into Franz's diffusion cell so that the mucosal membrane facing donor compartment and other side bathed in receptor compartment media. An aliquots of PTX-UDNVs dispersion and plain drug suspension equivalent to 5 mg PTX were added to the donor compartments of each cell. The diffusion cell assemblies maintained at 37 ± 1 °C and the contents of the receptor compartments were constantly stirred at 100 rpm. Samples were withdrawn (1 ml) via the sampling port at 2, 4, 6, 8, 10, 12 and 24 h and replenished with equal volume of fresh medium to maintain sink condition throughout the experiment. Cumulative amount permeated per cm^2 surface area of vaginal membrane was calculated and plotted against time. The transdermal steady-state flux (JSS; µg/cm^2/h) was calculated from the slope of the terminal linear portion of this graph.

Vaginal membrane deposition of the drug was measured at the end of the permeation experiments. The surface of the vaginal membrane was thoroughly washed with five aliquots of 50% methanol to remove excess drug from the surface. The vaginal membrane was then cut into small pieces. The tissue was further homogenized with 70% methanol and left for 24 h at room temperature. The homogenized tissue mass was shaken and centrifuged at 3500 rpm for 5 min and the content of PTX was determined in the supernatant.

7.3.1.7. Physical stability of PTX-UDNVs in IVR

Physical stability of the PTX-UDNVs in IVR lyophilized matrix was evaluated by re-dispersing the lyophilized content of IVR in pre-filtered triple distilled water. The resulting dispersion was evaluated for vesicle size and entrapment efficiency using the methods described in previous sections.

7.3.2. Results and Discussion

7.3.2.1. Vesicle Size and Zeta Potential

The vesicle size and zeta potential of the optimized formulation were measured in the triplicates and the results were 214.2 ± 4.22 nm and -34.3 ± 2.32 mV respectively. Vesicle size is an important parameter and determining factor in drug release kinetics, fluidity of the lipid bilayer and thereby stability of the formulation [5]. Polydispersity index (PDI) is used as a measure of broadness of vesicle size distribution. The optimized formulation showed PDI less than 0.2 which clearly indicates that the size distribution of the vesicles in the developed formulation was uniform [6].

		Diam. (nm)	% Intensity	Width (nm)
Z-Average (d.nm): 213.3	Peak 1:	234.0	100.0	93.95
PdI: 0.153	Peak 2:	0.000	0.0	0.000
Intercept: 0.893	Peak 3:	0.000	0.0	0.000
Result quality : Good				

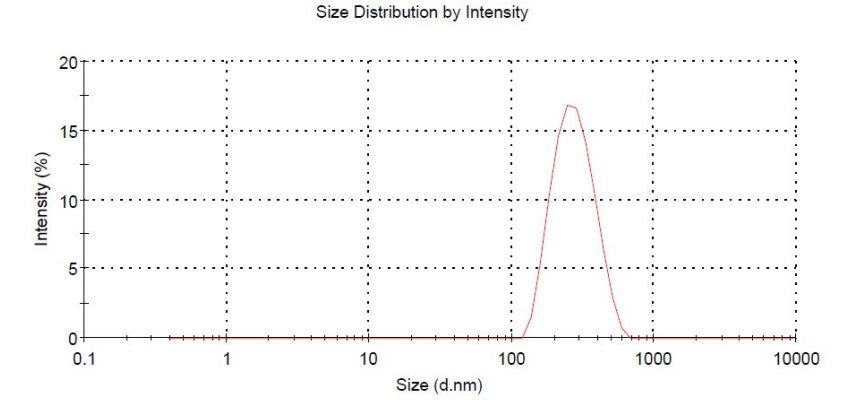

Fig. 7-1: PTX-UDNVs vesicle size analysis

		Mean (mV)	Area (%)	Width (mV)
Zeta Potential (mV): -34.9	Peak 1:	-34.9	100.0	5.61
Zeta Deviation (mV): 5.61	Peak 2:	0.00	0.0	0.00
Conductivity (mS/cm): 0.0093	Peak 3:	0.00	0.0	0.00
Result quality : Good				

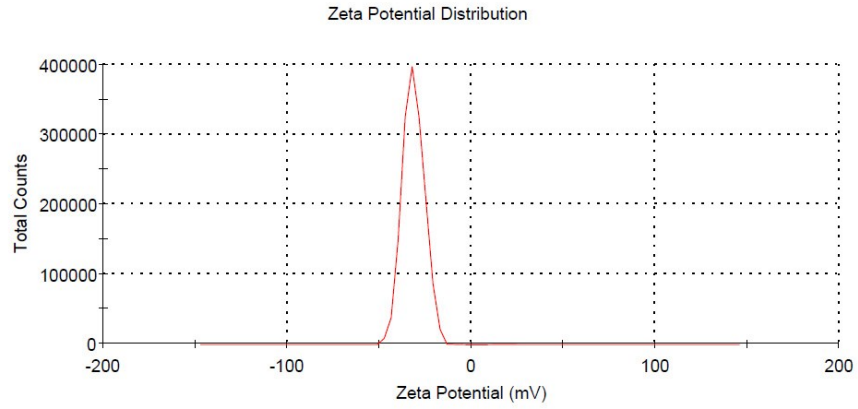

Fig. 7-2: PTX-UDNVs surface charge (zeta potential) analysis

Determination of zeta potential express the overall charge of vesicle attained in a specific medium. Its practical implication is to allow the quantification of the electrostatic repulsion between the vesicles, which is one of the most important forces controlling the behaviour and physical stability of vesicular dispersion [7]. Additionally, zeta potential of the formulation provides valuable information related to their in vivo functioning as the surface charge is an important element for their clearance from the general circulation and their tissue deposition [8]. The membrane surface potential

also plays key role in the aggregation and fusion of the vesicles and hence in the physical stability of the formulation. The higher value of the zeta potential obtained in the present study could be due to the anionic nature of sodium deoxycholate.

7.3.2.2. Entrapment efficiency and Drug loading

Drug Entrapment Efficiency and loading of the optimized formulation were found to be 91.27 ± 1.26 % and 8.92 ± 0.12 % respectively for three replicate batches (n=3). The reason for high %EE achieved is due to the use of DSPC lipid. DSPC with higher phase transition temperature and long acyl chains generally exhibit greater stability and is capable of sustaining entrapped molecule with less leakage from the vesicles. PTX being a lipophilic drug exhibits higher affinity towards lipophilic fatty acid chain lengths of the DSPC lipid and gets loaded within the lipid bilayers with high efficiency as well as improved loading capacity [9]. In the presence of rigid acyl chain of DSPC, freedom of movement of lipophilic chains decreases and this may lead to lower drug-membrane interaction and significantly lower drug leakage from the vesicles.

7.3.2.3. Deformability of the vesicles

The flexibility of the lipid bilayer is an important parameter to be evaluated for understanding of the interrelationship between vesicle permeation in biological tissues and composition of the formulation and the set process parameters. The optimized PTX-UDNVs formulation exhibited DI of the 25.61 ± 1.18 whereas the conventional liposome showed DI of 6.73 ± 1.66. The DI of the UDNVs formulation was found to be 3.8 times higher than that of conventional liposomes. This high membrane deformability is achieved probably by combining lipophilic and amphiphilic components (lipids & edge activators), with sufficiently different packing characteristics, into a single bilayer [10]. The presence of edge activator in the lipid bilayer imparts fluidity in the membrane which ultimately deforms to penetrate from the pores present in the biological membrane. These ultra-deformable vesicles consequently, undergo shape changes, whenever deformations are enforced by surrounding stress or space confinements, which minimizes the risk of vesicle rupture upon penetrating the pores [11].

7.3.2.4. Shape and surface morphology using TEM

Nano-sized vesicles can be effectively analysed for their shape and surface characteristics using transmission electron microscopy (TEM) technique. The transmission electron microscope is a very powerful tool which can be used to study and analyse the quality, shape, size of the vesicles, crystal structures, growth of layers, their composition etc. TEM can also be used to study lamellarity of the vesicles.

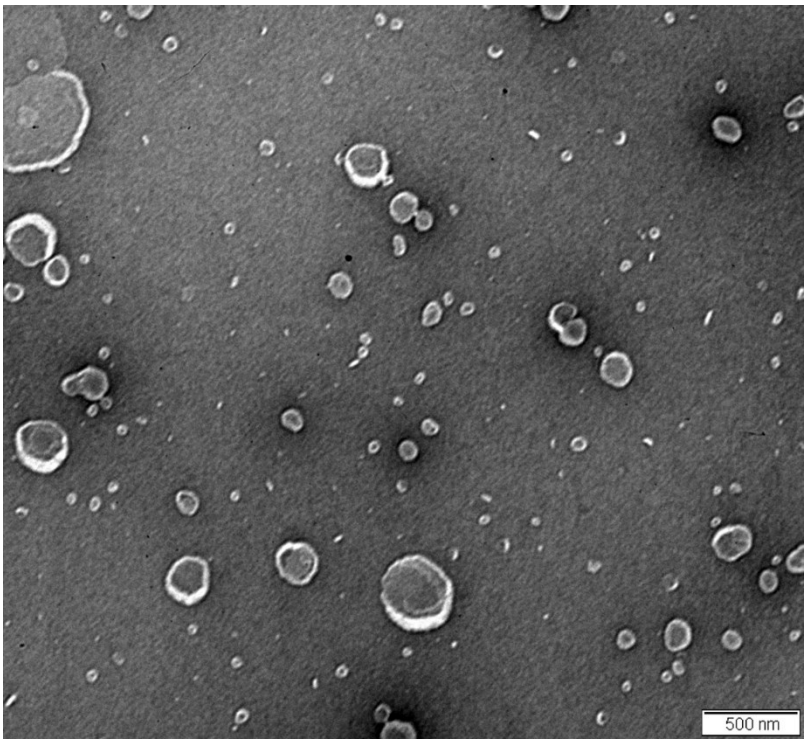

Fig. 7-3: Transmission electron microscopic image of optimized PTX-UDNVs

Fig. 7-3 represents image of TEM of the optimized PTX-UDNVs formulation. The image shows that the vesicles were spherical and smooth boundaries & not showing any aggregation. The size of vesicles seen in the image was found in good agreement with the results of vesicle size data obtained from Malvern size analyser.

7.3.2.5. In Vitro drug release study

The drug release behaviour of PTX-UDNVs and Plain drug suspension was studied. In Vitro drug release (% CDR) of PTX-UDNVs and Plain Drug Suspension over predetermined time points was plotted in **Fig. 7-4**. The initial time-points showed that the drug release from the plain drug suspension was considerably faster than that of the UDNVs formulation which exhibited highly controlled behaviour of the drug

release. More than 95% of the drug was released within 18 h in the case of plain drug suspension whereas UDNVs formulation was able to sustain drug release for more than 144 h (~6 days). In last couple of decades, mathematical modelling of drug release is being attempted to develop apt drug carriers with preferred drug release while they are at the target site [12]. Release kinetics models mainly form a predictability of the temporal drug release in vivo along with enhanced understanding of the release mechanism and a specific pattern of drug release. Most of the models are predicated on the basis of diffusion equations depending upon composition and conditions of release [13, 14]. Various mathematical models were applied to understand the release kinetics of PTX from the UDNVs. The release from PTX-UDNVs was found to follow zero order kinetics with R^2 = 0.985.

Table 7-1: In Vitro drug release of PTX-UDNVs and Plain Drug Suspension

Time (h)	% CDR (n=3)	
	PTX-UDNVs	Drug Suspension
1	3.66 ± 0.17	3.38 ± 0.14
2	3.86 ± 0.18	14.42 ± 1.07
3	5.42 ± 0.16	48.15 ± 6.70
4	5.59 ± 0.13	57.17 ± 6.33
6	5.65 ± 0.12	74.00 ± 5.46
8	5.91 ± 0.03	90.10 ± 6.27
10	6.90 ± 0.25	94.06 ± 3.28
12	7.67 ± 0.21	94.75 ± 3.50
18	8.10 ± 0.16	95.78 ± 3.43
24	10.14 ± 0.02	98.24 ± 2.94
36	19.81 ± 0.88	
48	31.75 ± 1.16	
72	47.77 ± 1.13	
96	72.09 ± 1.12	
120	92.45 ± 2.03	
144	97.67 ± 2.25	

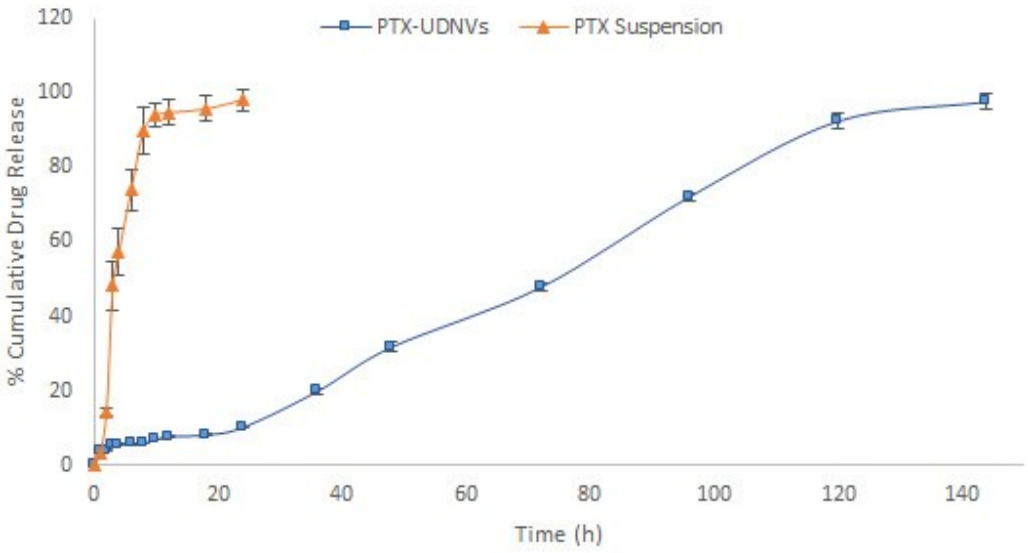

Fig. 7-4: In Vitro drug release of PTX-UDNVs and Plain Drug Suspension

As reviewed by A Jain et al [14] zero order drug release kinetics can be useful for transdermal drug delivery, ocular drug delivery and delivery of drugs with low water solubility. Zero order pattern of release may be desired for slow and prolonged delivery of antibiotics, antidepressants, maintenance of blood pressure, pain management and cancer therapy.

Table 7-2: In Vitro drug release of PTX-UDNVs loaded IVR

Time (h)	% CDR (n=3) PTX-IVR
1	2.92 ± 0.60
2	3.26 ± 0.67
3	4.76 ± 1.02
4	5.33 ± 1.21
6	5.72 ± 1.33
8	6.23 ± 1.98
10	7.39 ± 1.26
12	8.23 ± 1.25
18	13.75 ± 1.31
24	19.47 ± 2.5
36	33.71 ± 2.51

48	44.67 ± 1.46
72	66.12 ± 2.18
96	82.39 ± 2.33
120	95.33 ± 2.42

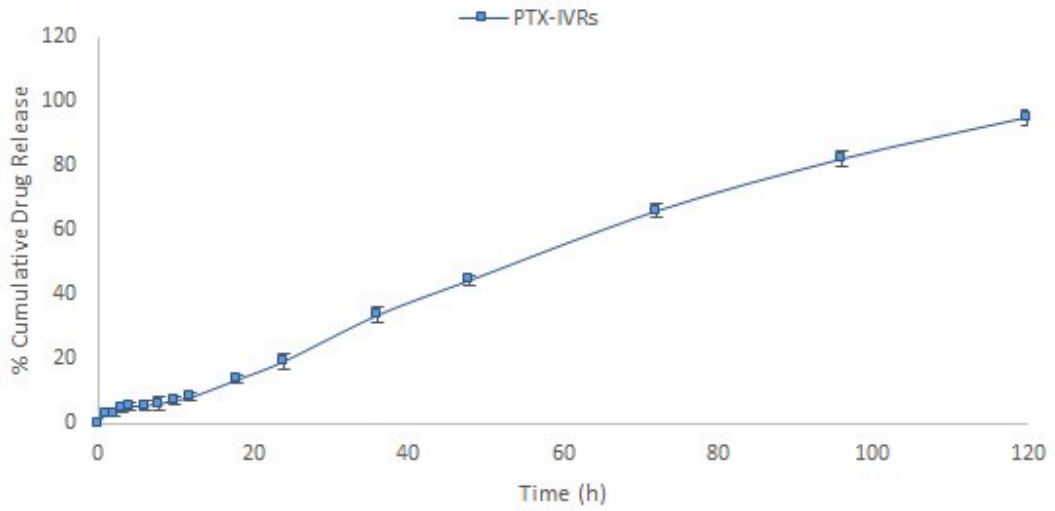

Fig. 7-5: In Vitro drug release profile of PTX-UDNVs from IVR

Drug release profile from the PTX-UDNVs loaded IVR was plotted in **Fig. 7-5**. PTX release from the IVR was found to be in highly controlled fashion i.e. around 95% of the drug was released in 120 h (~5 days). The drug release behaviour was almost similar to that of PTX-UDNVs dispersion. Moreover, the drug release kinetics was found to fit zero order model with R^2 of 0.992 amongst various mathematical models applied which further suggests similarity of the release behaviour. The obtained results are in agreement with the reported research by Celia, C. et al [15] regarding two weeks prolonged drug release following zero order which resulted into enhanced anticancer potential as passive targeting exhibited by nano carriers while maintaining constant accumulation in breast cancer cells.

7.3.2.6. Permeation and Deposition study

Permeation study through vaginal membrane was conducted with the PTX-UDNVs formulation and plain drug suspension by using diffusion cell. This ex vivo method is

commonly used in transdermal drug delivery research to obtain valuable information about the formulation behaviour in vivo. **Table 7-3** summarizes the cumulative amount of PTX permeated per cm^2 area of vaginal membrane, steady state flux (Jss) and % drug permeated after 24 h for UDNVs formulation and plain drug suspension.

Table 7-3: Drug permeation profile of PTX-UDNVs and Plain drug suspension

Time (h)	Drug Permeation (µg/cm^2)	
	PTX-UDNVs	**Plain drug**
1	21.77±11.33	11.88±2.03
2	135.32±13.68	14.18±6.48
3	212.45±32.86	16.64±4.64
4	278.36±34.78	29.88±8.57
6	591.54±38.21	48.51±16.84
8	1037.54±61.32	60.04±12.52
10	1167.32±30.71	111.18±30.98
12	1316.54±41.47	166.94±33.64
18	1386.94±44.03	199.06±45.16
24	1460.75±45.16	257.45±31.73
Jss	12.02	7.54
% Drug Permeation after 24 h	55.51±1.72	9.78±1.21

The total amount of drug penetrated through the vaginal membrane after 24 h were 1460.75±45.16 & 257.45±31.73 µg/cm^2 in the case of PTX-UDNVs and Plain drug suspension respectively. The value of Jss for PTX-UDNVs was 1.6 times higher than that of plain drug. Moreover, the % drug permeation after 24 h was 5.7 times high than that of plain drug. The higher values of transmembrane flux and % drug permeation

for PTX-UDNVs were indicative of enhanced penetration capabilities of the formulation compared to the plain drug suspension.

7.3.2.7. Physical stability of PTX-UDNVs in IVR

The results for vesicle size and entrapment efficiency of PTX-UDNVs after re-dispersion were compared with the initial values as tabulated in **Table 7-4**.

Table 7-4: Vesicle size and Entrapment of PTX-UDNVs initially and after re-dispersion of IVR

Parameters	PTX-UDNVs	
	Initial	Re-dispersion
% EE	91.45 ± 1.39	90.76 ± 2.25
Vesicle Size (nm)	217.1 ± 2.67	225.5 ± 3.03

There was no significant difference observed in mean vesicle size and entrapment efficiency of the UDNVs indicating their stability within lyophilized matrix of IVRs.

7.4. Characterization of CBP-UDNVs

7.4.1. Methods

7.4.1.1. Vesicle Size and Zeta Potential

Briefly, vesicular dispersion was taken (50 µL) and diluted it with 2 ml of distilled water in order to obtain proper vesicle density. The dispersion thus prepared was filled in clear disposable sizing cuvettes and the mean hydrodynamic diameter and poly-dispersity index (PDI) were measured in triplicate by dynamic light scattering using Nano-ZS zetasizer. For the measurement of Zeta Potential, the diluted dispersion was transferred to disposable folded capillary cells and analysed for zeta potential using Nano-ZS zetasizer.

7.4.1.2. Entrapment efficiency and Drug loading

The vesicular dispersion was taken in centrifuge tubes and centrifuged at 20,000 rpm at 4 °C for 1hr. The pellet settles down while free drug remains in the supernatant. The pellet was separated from the supernatant and lysed using 1% Triton X100 solution.

The contents were suitably diluted and analysed using the developed HPLC method. The entrapment efficiency and drug loading were calculated using following formula-

$$\%\ Entrapment\ Efficiency\ = \frac{Estimated\ Entrapped\ drug}{Total\ drug\ added\ to\ formulation} \times 100$$

$$\%\ Drug\ Loading\ (\%w/w) = \frac{Estimated\ Entrapped\ drug}{Total\ weight\ of\ the\ formulation} \times 100$$

7.4.1.3. Deformability of the vesicles

The deformability of the phospholipid bilayer of CBP-UDNVs formulation and conventional liposomes was assessed using membrane extrusion method. Vesicular dispersion was diluted using double distilled water to obtain final volume of 50 ml. The diluted formulations were extruded at constant pressure through the 25 mm diameter Isopore polycarbonate filter membrane having a pore diameter of 100 nm. The amount of vesicle dispersion that was extruded during 5 min was measured, and the vesicle was monitored before and after extrusion [2].

The deformability of the nano-vesicles was measured using following equation:

$$DI = J \times \left(\frac{R_v}{R_p}\right)^2$$

Where, *DI*= Deformability Index;

J= Amount of dispersion extruded (ml);

R_v= Vesicles size after extrusion (nm); and

R_p= Pore size of the barrier (nm)

7.4.1.4. Shape and surface morphology using TEM

The optimized formulation was evaluated for morphological properties using transmission electron microscopy (TEM). The vesicular dispersion was spread on a carbon-coated grid, excess solution was removed and the grid was dried under infrared lamp. 2% phosphotungstic acid (PTA) was used for negative staining and again

dried under Infrared lamp. Transmission electron microscope (CM 200, Philips, Netherlands) with operating voltage range of 20-200 kV was used to visualize vesicles at suitable enlargement with an accelerating voltage of 20 kV.

7.4.1.5. In Vitro drug release study

Drug release from the CBP loaded UDNVs was studied using dialysis bag technique in phosphate buffer pH 4.5. The aqueous UDNVs dispersion equivalent to 10 mg of drug was placed in activated dialysis membrane (MWCO- 12000, Hi media, India) closed as one end by clamp. The other end was also closed using clamp and whole bag was immersed in a beaker containing 50 ml phosphate buffer pH 4.5 which was stirred at 100 rpm and maintained at 37 ± 1 °C throughout the experiment. At predetermined time intervals, 1 ml samples were withdrawn from the receptor compartment and sink conditions were maintained by addition of similar quantities of fresh media. The samples were analysed for amount of drug released using previously described HPLC method [3]. All the experiments were performed in triplicate, and the average values were considered. Drug release from the plain drug solution was also studied in the similar manner and used as control for comparison.

In vitro drug release from Intra Vaginal Rod (IVR) inserts was also performed in similar method as described above. The IVR containing freeze-dried rod of the formulation was placed in the diffusion medium (phosphate buffer pH 4.5) maintained at 37 ± 1 °C and 100 rpm speed was kept constant. 1 ml samples were withdrawn from the receptor compartment (media) and sink conditions were maintained by addition of fresh media. The samples were analysed for amount of drug released using previously described HPLC method. All the experiments were performed in triplicate.

7.4.1.6. Permeation and Deposition Study

The permeation of CBP-UDNVs and plain drug solution was determined across Porcine Vaginal Membrane. The porcine vaginal tissue was obtained immediately after animal sacrifice in a local slaughterhouse and preserved in the isotonic sodium chloride solution. Tissue was rinsed three times with saline solution, separated from the underneath connective tissues, and mounted between donor and receptor

compartment of Franz's diffusion cell with 1.9 cm^2 effective diffusion area and 15 mL receptor chamber volume. The receptor compartment was filled with PBS (pH 7.4) with constant stirring at 100 rpm. The vaginal membrane was carefully mounted into Franz's diffusion cell so that the mucosal membrane facing donor compartment and other side bathed in receptor compartment media. An aliquots of CBP-UDNVs dispersion and plain drug solution equivalent to 10 mg CBP were added to the donor compartment. The cell assembly was maintained at 37 ± 1 °C and the contents of the receptor compartment were constantly stirred at 100 rpm. Samples were withdrawn (1 ml) via the sampling port at 2, 4, 6, 8, 10, 12 and 24 h and replenished with equal volume of fresh medium to maintain sink condition throughout the experiment [4]. Cumulative amount permeated per cm^2 surface area of vaginal membrane was calculated and plotted against time. The transdermal steady-state flux (JSS; $\mu g/cm^2/h$) was calculated from the slope of the terminal linear portion of this graph.

Vaginal membrane deposition of the drug was measured at the end of the permeation experiments. The surface of the vaginal membrane was thoroughly washed with five aliquots of the distilled water to remove excess drug from the surface. The vaginal membrane was then cut into small pieces. The tissue was further homogenized with 10% methanol and left for 24 h at room temperature. The homogenized tissue mass was shaken and centrifuged at 3500 rpm for 5 min and the content of CBP was determined in the supernatant.

7.4.1.7. Physical stability of CBP-UDNVs in IVR

Physical stability of the CBP-UDNVs in IVR lyophilized matrix was evaluated by re-dispersing the lyophilized content of IVR in pre-filtered triple distilled water. The resulting dispersion was evaluated for vesicle size and entrapment efficiency using the methods described in previous sections.

7.4.2. Results and Discussion

7.4.2.1. Vesicle Size and Zeta Potential

The vesicle size and zeta potential of the optimized formulation were measured in the triplicates and the results were 293.7 ± 3.17 nm and -28.1 ± 1.54 mV respectively.

Vesicle size is an important parameter and determining factor in drug release kinetics, fluidity of the lipid bilayer and thereby stability of the formulation. Polydispersity index (PDI) is used as a measure of broadness of vesicle size distribution. The optimized formulation showed PDI less than 0.2 which clearly indicates that the size distribution of the vesicles in the developed formulation was uniform.

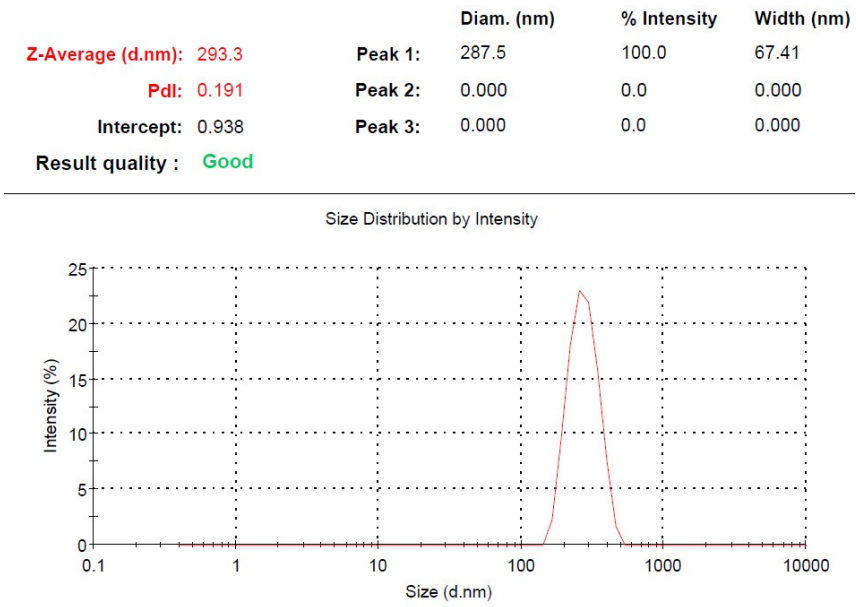

Fig. 7-6: CBP-UDNVs vesicle size analysis

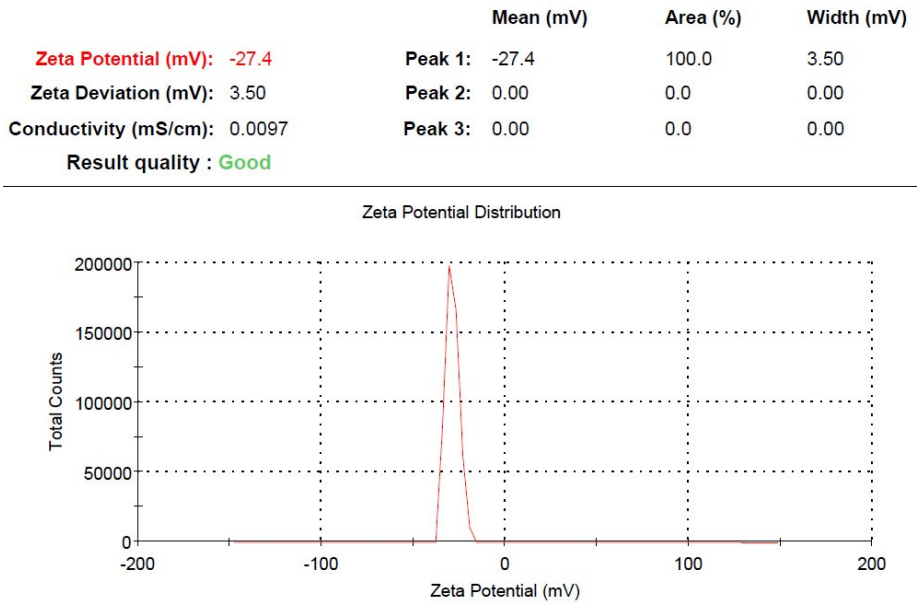

Fig. 7-7: CBP-UDNVs surface charge (zeta potential) analysis

Determination of zeta potential express the overall charge of vesicle attained in a specific medium. Its practical implication is to allow the quantification of the electrostatic repulsion between the vesicles, which is one of the most important forces controlling the behaviour and physical stability of vesicular dispersion. Additionally, zeta potential of the formulation provides valuable information related to their in vivo functioning as the surface charge is an important element for their clearance from the general circulation and their tissue deposition. The membrane surface potential also plays key role in the aggregation and fusion of the vesicles and hence in the physical stability of the formulation. The higher value of the zeta potential obtained in the present study could be due to the anionic nature of sodium deoxycholate.

7.4.2.2. Entrapment efficiency and Drug loading

Drug Entrapment Efficiency and loading of the optimized formulation were found to be 68.79 ± 2.04 % and 8.22 ± 0.24 % respectively for three replicate batches (n=3). The probable reason behind higher entrapment and loading of CBP- a hydrophilic molecule – could be good packing between lipids and edge activator molecules simultaneously providing fluidity to the membrane. Curing of the vesicular dispersion above its transition temperature, resulted into more drug penetration in lipid bilayer and getting entrapped into the vesicles by enhanced membrane permeability. Moreover concentration gradient generated while reduction in hydration volume might have played an important role in higher entrapment and loading of CBP.

7.4.2.3. Deformability of the vesicles

The deformability is a crucial and unique parameter of UDNVs as it differentiates them from other lipid vesicles that are unable to cross intact biological membranes. The optimized CBP-UDNVs formulation exhibited DI of the 89.13 ± 3.44 whereas the conventional liposome showed DI of 17.89 ± 4.33. The DI of the UDNVs formulation was found to be five times higher than that of conventional liposomes. The exceptional deformability of the lipid bilayer membrane probably achieved by combination of dual lipids and use of sodium deoxycholate as an edge activator which might have played an important role in rendering vesicles more flexible. Moreover, drug molecule being

hydrophilic in nature, the entrapment of the drug would be more prominent in hydrophilic core of the vesicles. This might have reduce load in lipid bilayer thereby helping the lipid bilayer to adapt even more flexibility.

7.4.2.4. Shape and surface morphology using TEM

TEM works by focusing the beam of electrons from the electron gun into a small, thin, coherent beam by the use of the condenser lens and aperture which restricts & excludes high angle electrons from the beam. The beam then strikes the specimen and parts of it are transmitted depending upon the thickness and electron transparency of the specimen which is then focused by the objective lens into an image on phosphor screen or charge coupled device (CCD) camera hence light is generated, allowing the user to see the image. The darker areas of the image represent those areas of the sample that fewer electrons are transmitted through while the lighter areas of the image represent those areas of the sample that more electrons were transmitted through.

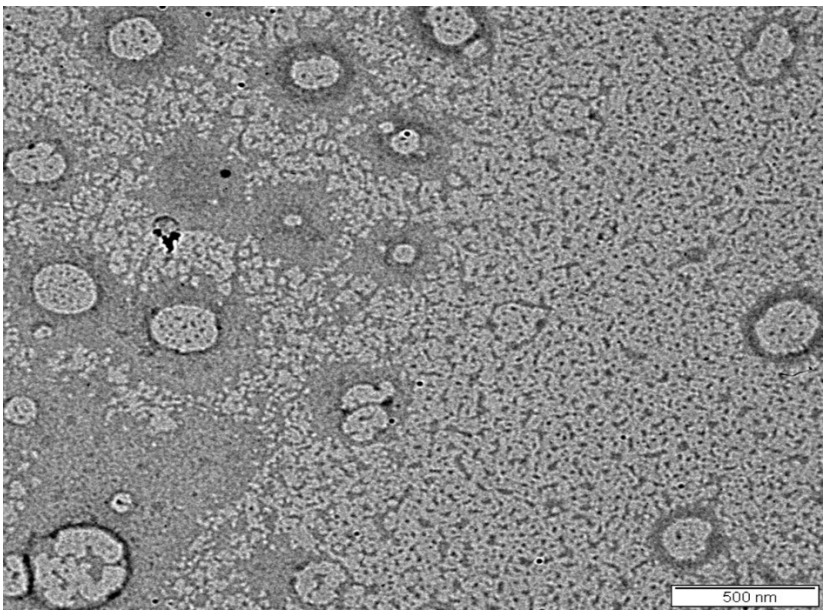

Fig. 7-8: Transmission electron microscopic image of optimized CBP-UDNVs

The TEM image of the optimized formulation was represented in **Fig. 7-8**. The image shows spherical and smooth vesicular boundaries with no signs of aggregation. Moreover, the size of the vesicles observed in the image was found to be in agreement with the results of vesicle size range obtained from the Malvern Zetasizer.

7.4.2.5. In Vitro drug release study

To predict performance of UDNVs in vivo, good in vitro models that can determine the release kinetics from UDNVs at the early stage of the formulation development process are necessary. The drug release behaviour of CBP-UDNVs and Plain drug solution was studied. In Vitro drug release (% CDR) of CBP-UDNVs and Plain Drug Solution over predetermined time points was plotted in **Fig. 7-9**. The initial time-points showed that the drug release from the plain drug solution was considerably faster than that of the UDNVs formulation which exhibited highly controlled behaviour of the drug release. Almost all the drug amount was released within 8 h in the case of plain drug solution whereas UDNVs formulation was able to sustain drug release for more than 120 h (~5 days). 98.07 % of drug was released after 120 h in the case of CBP-UDNVs whereas more than 95 % of the drug was released within 6 h from the plain drug solution of CBP. Various mathematical models, applied to understand the release kinetics of CBP from the UDNVs. It was found that drug release from CBP-UDNVs followed zero order kinetics with R^2 of 0.991.

Table 7-5: In Vitro drug release of CBP-UDNVs and Plain Drug Solution

Time (h)	% CDR (n=3)	
	CBP-UDNVs	**Drug Solution**
1	1.31 ± 0.04	12.73 ± 1.47
2	2.89 ± 0.11	28.62 ± 1.61
3	4.37 ± 0.14	35.38 ± 4.69
4	4.81 ± 0.11	49.97 ± 3.06
6	5.96 ± 0.21	95.55 ± 1.42
8	7.47 ± 1.04	99.64 ± 0.28
10	9.42 ± 1.91	
12	10.73 ± 1.45	
18	12.55 ± 2.23	
24	14.64 ± 2.38	

36	23.67 ± 2.67	
48	37.12 ± 2.87	
72	63.89 ± 2.43	
96	84.37 ± 2.12	
120	98.07 ± 1.71	

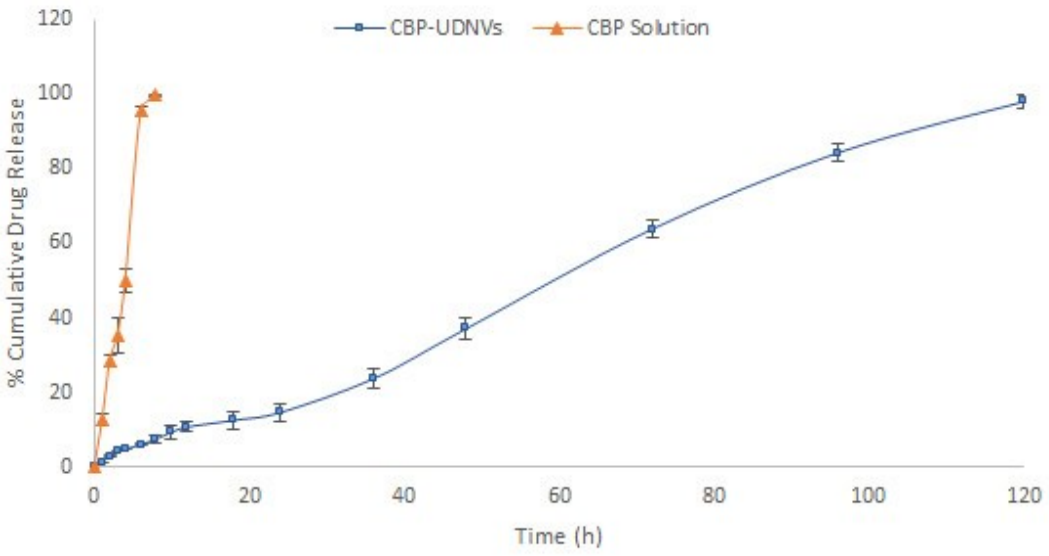

Fig. 7-9: In Vitro drug release of CBP-UDNVs and Plain Drug Solution

The results of release of CBP – a hydrophilic molecule – from UDNVs formulation are in agreement with the other hydrophilic small molecules formulation as reported by S.H. Kiaie, et al. [16]. Authors report that the slow leakage of drug from the formulation results into lower volume of distribution than the free drug which indicates that drug loaded formulation may exist in the circulation until extravasate to tumor tissue or uptake by RES with less toxicity that the free drug.

Table 7-6: In Vitro drug release of CBP-UDNVs loaded IVR

Time (h)	**% CDR (n=3) CBP-IVR**
1	1.29 ± 0.57

2	2.76 ± 0.84
3	3.98 ± 0.81
4	4.67 ± 0.99
6	5.87 ± 1.55
8	8.01 ± 1.51
10	9.94 ± 1.05
12	10.89 ± 1.61
18	17.45 ± 1.67
24	23.22 ± 1.77
36	37.76 ± 1.86
48	49.56 ± 2.02
72	74.94 ± 2.69
96	92.57 ± 2.06
120	97.21 ± 2.15

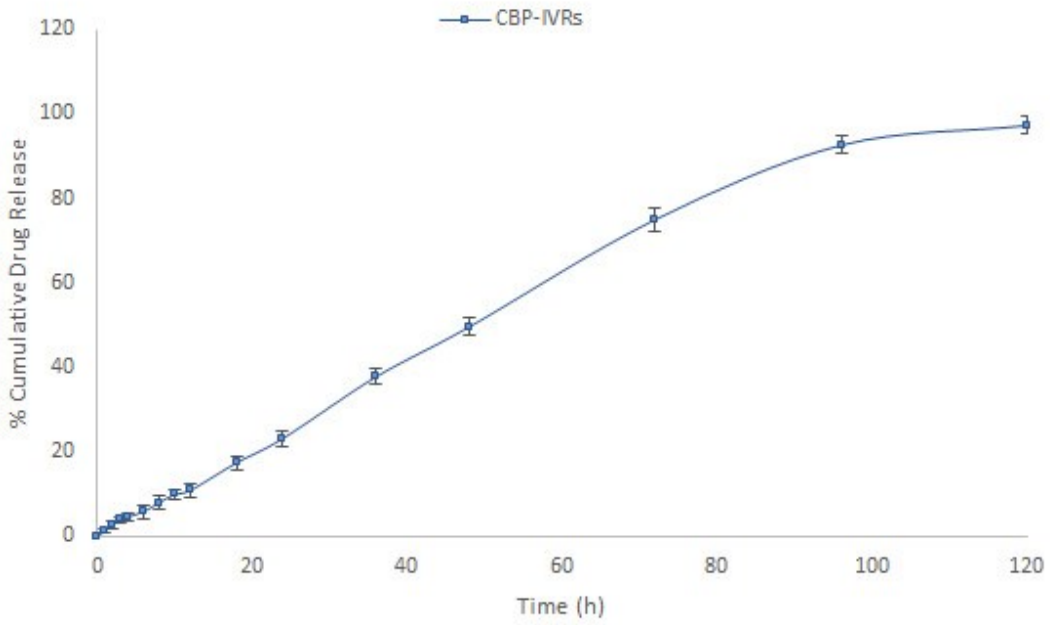

Fig. 7-10: In Vitro drug release profile of CBP-UDNVs from IVR

Drug release profile from the CBP-UDNVs loaded IVR was plotted in **Fig. 7-10**. CBP release from the IVR was found to be in highly controlled fashion i.e. 92.57% of the drug was released in 120 h (~5 days). The drug release behaviour was almost similar to that of CBP-UDNVs dispersion. Moreover, the drug release kinetics was found to fit Korsmeyer-Peppas model with R^2 of 0.995 and n = 0.92 amongst various mathematical models applied which further suggests resemblance of the release behaviour. In Korsmeyer-Peppas model, n is the diffusional exponent for drug release. The diffusional exponent, n, is dependent on the geometry of the release source as well as the physical mechanism for release. The values of n for the case of cylindrical devices, $0.45 \leq n$ corresponds to a Fickian diffusion mechanism, $0.45 < n < 0.89$ to non-Fickian transport, n = 0.89 to Case II transport, and n > 0.89 to super case II transport or zero-order release in this model. For systems exhibiting case II transport, the dominant mechanism for drug transport is due to polymer matrix relaxation. The value of n > 0.43 but < 0.85 is considered as anomalous transport (non-Fickian) and refers to the coupling of Fickian diffusion and polymer matrix relaxation. The value of n > 0.85 is considered as super case II transport which implies super case II release kinetics (a strong indication of zero order). Zero-order release is the ideal in controlled drug release and has been reported not to be common with matrix systems, this being attributed to time-dependant changes in drug matrix surface area and diffusional path length [17, 18].

7.4.2.6. Permeation and Deposition Study

Transmembrane permeation study of CBP-UDNVs formulation and plain drug solution was conducted using diffusion cell mounted with porcine vaginal tissue. This ex vivo method is commonly used in transdermal drug delivery research to obtain valuable information about the formulation behaviour in vivo. **Table 7-7** summarizes the cumulative amount of CBP permeated per cm^2 area of vaginal membrane, steady state flux (Jss) and % drug permeated after 24 h for UDNVs formulation and plain drug solution.

Table 7-7: Drug permeation profile of CBP-UDNVs and Plain drug solution

Time (h)	Drug Permeation (µg/cm^2)	
	CBP-UDNVs	**Plain drug**
1	14.41±7.22	11.37±2.9
2	59.17±12.32	12.04±8.15
3	193.25±25.46	16.37±6.01
4	409.56±39.64	22.25±14.06
6	602.67±22.81	43.87±22.22
8	673.27±46.97	69.52±29.15
10	727.26±18.17	99.84±18.51
12	798.58±60.76	111.68±42.66
24	1109.24±92.8	164.07±38.83
Jss	25.89	4.37
% Drug Permeation after 24 h	21.08±1.76	3.12±0.74

The total amount of drug penetrated through the vaginal membrane after 24 h were 1109.24±92.8 & 164.07±38.83 µg/cm^2 in the case of CBP-UDNVs and Plain drug solution respectively. The value of Jss for CBP-UDNVs was 5.9 times higher than that of plain drug. Moreover, the % drug permeation after 24 h was 6.8 times high than that of plain drug. The higher values of transmembrane flux and % drug permeation for CBP-UDNVs were indicative of enhanced penetration capabilities of the formulation compared to the plain drug solution.

The higher value of transmembrane flux for CBP-UDNVs was indicative of enhanced penetration capabilities of the formulation compared to the plain drug solution. The process of vesicle penetration is attributed to the high deformability, resulting from EA molecules accumulating at the site of high stress, due to their raised propensity for

greatly curved structures. Thus, vesicles undergo a series of stress-dependant adjustments of the local carrier composition, to minimize the resistance to their motion through the otherwise confining channels, which allows them to transport drugs noninvasively.

7.4.2.7. Physical stability of CBP-UDNVs in IVR

The results for vesicle size and entrapment efficiency of CBP-UDNVs after re-dispersion were compared with the initial values as tabulated in **Table 7-8**.

Table 7-8: Vesicle size and Entrapment of CBP-UDNVs initially and after re-dispersion of IVR

Parameters	CBP-UDNVs	
	Initial	Re-dispersion
% EE	67.88 ± 2.72	66.45 ± 3.11
Vesicle Size (nm)	297.5 ± 2.07	301.2 ± 2.83

There was no significant difference observed in mean vesicle size and entrapment efficiency of the UDNVs indicating their stability within lyophilized matrix of IVRs.

References:

1. Yang, T., et al., *Enhanced solubility and stability of PEGylated liposomal paclitaxel: in vitro and in vivo evaluation.* International journal of Pharmaceutics, 2007. **338**(1-2): p. 317-326.
2. Singh, H.P., et al., *Elastic liposomal formulation for sustained delivery of colchicine: in vitro characterization and in vivo evaluation of anti-gout activity.* The AAPS journal, 2009. **11**(1): p. 54-64.
3. Ravar, F., et al., *Hyaluronic acid-coated liposomes for targeted delivery of paclitaxel, in-vitro characterization and in-vivo evaluation.* Journal of Controlled Release, 2016. **229**: p. 10-22.
4. Wavikar, P. and P. Vavia, *Nanolipidgel for enhanced skin deposition and improved antifungal activity.* AAPS PharmSciTech, 2013. **14**(1): p. 222-233.

5. Iizhar, S.A., et al., *In vitro assessment of pharmaceutical potential of ethosomes entrapped with terbinafine hydrochloride.* Journal of advanced research, 2016. **7**(3): p. 453-461.
6. Maguire, C.M., et al., *Characterisation of particles in solution–a perspective on light scattering and comparative technologies.* Science and technology of advanced materials, 2018. **19**(1): p. 732-745.
7. Junyaprasert, V.B., V. Teeranachaideekul, and T. Supaperm, *Effect of charged and non-ionic membrane additives on physicochemical properties and stability of niosomes.* Aaps Pharmscitech, 2008. **9**(3): p. 851.
8. Lowry, G.V., et al., *Guidance to improve the scientific value of zeta-potential measurements in nanoEHS.* Environmental Science: Nano, 2016. **3**(5): p. 953-965.
9. Haeri, A., et al., *Preparation and characterization of stable nanoliposomal formulation of fluoxetine as a potential adjuvant therapy for drug-resistant tumors.* Iranian journal of pharmaceutical research: IJPR, 2014. **13**(Suppl): p. 3.
10. Hussain, A., et al., *Elastic liposomes as novel carriers: recent advances in drug delivery.* International journal of nanomedicine, 2017. **12**: p. 5087.
11. Parkash, V., et al., *Implementation of Design of Experiments in Development and Optimization of Transfersomal Carrier System of Tacrolimus for the Dermal Management of Psoriasis in Albino Wistar Rat.* J Bioequiv Availab, 2018. **10**: p. 99-106.
12. Lin, C.-C. and A.T. Metters, *Hydrogels in controlled release formulations: network design and mathematical modeling.* Advanced drug delivery reviews, 2006. **58**(12-13): p. 1379-1408.
13. Siepmann, J. and F. Siepmann, *Modeling of diffusion controlled drug delivery.* Journal of controlled release, 2012. **161**(2): p. 351-362.
14. Jain, A. and S.K. Jain, *In vitro release kinetics model fitting of liposomes: An insight.* Chemistry and physics of lipids, 2016. **201**: p. 28-40.
15. Celia, C., et al., *Sustained zero-order release of intact ultra-stable drug-loaded liposomes from an implantable nanochannel delivery system.* Advanced healthcare materials, 2014. **3**(2): p. 230-238.
16. Kiaie, S.H., et al., *Axial pharmaceutical properties of liposome in cancer therapy: Recent advances and perspectives.* International journal of pharmaceutics, 2020: p. 119269.
17. Ofokansi, K.C. and F.C. Kenechukwu, *Formulation development and evaluation of drug release kinetics from colon-targeted ibuprofen tablets based on Eudragit RL 100-chitosan interpolyelectrolyte complexes.* ISRN pharmaceutics, 2013. **2013**.

18. Fu, Y. and W.J. Kao, *Drug release kinetics and transport mechanisms of non-degradable and degradable polymeric delivery systems.* Expert opinion on drug delivery, 2010. **7**(4): p. 429-444.